

# Morphology of compacted polyethylene fibres

R. H. OLLEY, D. C. BASSETT

*J.J.Thomson Physical Laboratory, University of Reading, P O Box 220, Whiteknights, Reading RG6 2AF, UK*

P. J. HINE, I. M. WARD

*Interdisciplinary Research Centre in Polymer Science and Technology, University of Leeds, Leeds LS2 9JT, UK*

The microstructure of aggregates of parallel high-modulus polyethylene fibres, compacted at 138°C to give a composite with good mechanical properties, has been examined. Detail of transverse and longitudinal cross-sections has been revealed by permanganic etching and studied electron microscopically. The fibres pack together irregularly with coordination numbers typically between 4 and 7 and fibre diameters in the range 10–20 µm. Misalignment of fibres is generally close to zero but does occur incrementally, by 10° and more, between successive rows of fibres. A substantial proportion of fibres has deformed, often by shear, during treatment producing a broadening of interfibrillar contacts. A lamellar component of texture is present both between and within fibres. It is inferred to form by melting of those parts of the fibres where there is least constraint on the melt, followed by recrystallization on the fibres as nuclei. The lamellae therefore share the axial orientation of the fibres, while the crystallographic fibre/lamellar contact promotes good transverse properties.

## 1. Introduction

The composites of compacted polyethylene fibres whose preparation was reported in the previous paper [1] have been examined by optical and electron microscopy. The basic texture is one of contacting residual fibres joined together by stacks of lamellae which have nucleated on, and share a common chain (*c*) axis with, the fibrous skeleton. In addition there are gross variations due to misalignment of successive swathes of fibres and also different responses in different fibres to the treatment they have received. On a finer scale, the presence of lamellae is linked to the physical requirement of there having been room to melt rather than to variations of intrinsic composition in the original fibres. Finally, the etching techniques used, although not optimized for this purpose, already reveal significant and unexpected detail within the fibres, so that further study can confidently be expected to advance the understanding of structure/property relationships in polymeric fibres.

## 2. Experimental procedure

The compacted composite sample was in the form of a sheet 2.5 mm thick. Internal surfaces were exposed by cutting, at temperatures slightly below 0°C, with a diamond knife in a simple microtome. Cuts were made so as to reveal planes approximately perpendicular (transverse section) or parallel (longitudinal section)

to the average fibre axis. These exposed surfaces were either examined as prepared or, in most cases, after etching with a permanganic reagent. Experience shows that different reagents are required to optimize detail in different components of texture. That used for most of the work was 1% wt/vol potassium permanganate dissolved by continuous stirring in an acidic mixture consisting of 10 volumes sulphuric acid, 4 volumes orthophosphoric acid (BDH reagent, minimum 85%), 1 volume water, the sample being shaken for 2 h in the mixture.

For Fig. 3 the acidic mixture was 10 volumes sulphuric acid, 4 volumes orthophosphoric acid (BDH reagent, minimum 85%), and 4 volumes water.

For Figs 7 and 9 a 2% wt/vol solution of potassium permanganate was used in a mixture of 2 volumes sulphuric acid, 1 volume orthophosphoric acid dried to boiling point 260°C, the sample being shaken for 4 h.

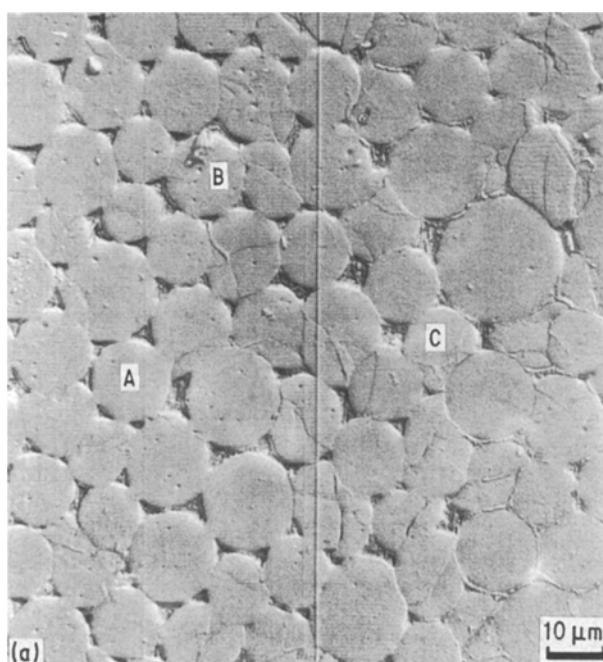
Recovery of etched specimens was as previously published [2], except that a small quantity of hydrogen peroxide was added to the chilled acid mixture, instead of being applied as a second step.

A standard two-stage replication process was used, first making an impression of the etched surface in softened cellulose acetate and then shadowing this first replica with tantalum–tungsten, followed by deposition of a carbon film, and extraction of the shadowed carbon replica [3].

### 3. Results and discussion

#### 3.1. General features

The appearance of a cross-section normal to the fibres is shown in Fig. 1. This shows the sample as cut, without etching; in consequence, faint knife marks are present running horizontally (parallel to the knife edge) together with the prominent vertical line (parallel to the cutting direction) in Fig. 1a. Several important points are already evident at this optical magnification. The two basic elements of texture, fibres and interfibrillar regions, are clearly distinguished. The fibres vary in diameter by a factor of about two, from  $\sim 10\ \mu\text{m}$  to  $> 20\ \mu\text{m}$ . Their packing has, therefore, to be irregular; coordination numbers of 4, 5, 6 and 7 are common. Interfibrillar connections sometimes have the appearance of necks similar to those which develop in sintered metals or ceramics (A, Fig. 1a) with no clear interfibrillar boundary visible. In such instances the cross-sections remain more or less circular. In other cases there is gross deformation. Thus to the right of B in Fig. 1a, a fibre has sheared through and conformed to the shapes of the adjacent fibres, with clear boundaries remaining between them. Sometimes, e.g. right of C in Fig. 1a, fibres have distorted very severely to fill the space where contacting circular cross-sections would have left interstices. Finally, there are reversals of contrast of the interfibrillar regions. That in the bottom right corner of Fig. 1a is the reverse of elsewhere in the micrograph, giving the impression of being proud of rather than below the ends of the fibres. A very striking example of such a change divides Fig. 1b in two, nearly vertically with a very prominent boundary accentuated by distortion of the contacting fibres. Similar features recur at intervals of  $\sim 0.1\ \text{mm}$  and become very prominent with certain etching treatments. They appear to represent consecutive tows in the laying down of the material, each with a slight change in the direction of the fibres.



#### 3.2 Organization of fibres

When specimens have been etched with a permanganic reagent, typically a few micrometres are removed selectively from exposed surfaces (including cutting damage) thereby revealing underlying detail. In Fig. 2, which is viewed obliquely (tilted  $60^\circ$  about a horizontal axis) to accentuate relief, there is a prominent central fibre of  $13\ \mu\text{m}$  diameter. This appears elliptical but is, in fact, effectively circular. Triangular interstices containing recrystallized lamellae are present between this fibre and its neighbours. The most prominent feature in Fig. 2 is, however, the extensive cratering which has developed on the exposed fibre ends. The significance of these craters, which have diameters to  $\sim 1\ \mu\text{m}$ , is unclear at this stage. Later it will be shown that they are not an artefact of the preparation procedures but do arise from a real textural feature. Etching may well have developed the relief but there is an underlying texture within the fibre which is its fundamental cause.

In a longitudinal section one intends to cut a plane parallel to the fibre axis, in which case the full length of the fibre will be seen. Should, however, the plane of the cut lie at an angle  $\theta$  to that of the fibre axis, then a right circular fibre will intersect the plane in an ellipse obeying the formula

$$\sin\theta = \text{minor axis length}/\text{major axis length} \quad (1)$$

Fig. 3 is a longitudinal section of the etched compacted fibres. On its left the fibres do extend over the height of the micrograph, i.e. they lie in the plane of the page. But on the right of Fig. 3 this is no longer the case and elliptical sections are seen, albeit foreshortened by a rotation of  $60^\circ$  around a horizontal axis. When the obliquity is taken into account the aspect ratio of the ellipses (major:minor axis lengths) is somewhat variable with typical values of  $\sim 5$  and a minimum of 3.5, implying that these fibres have axes

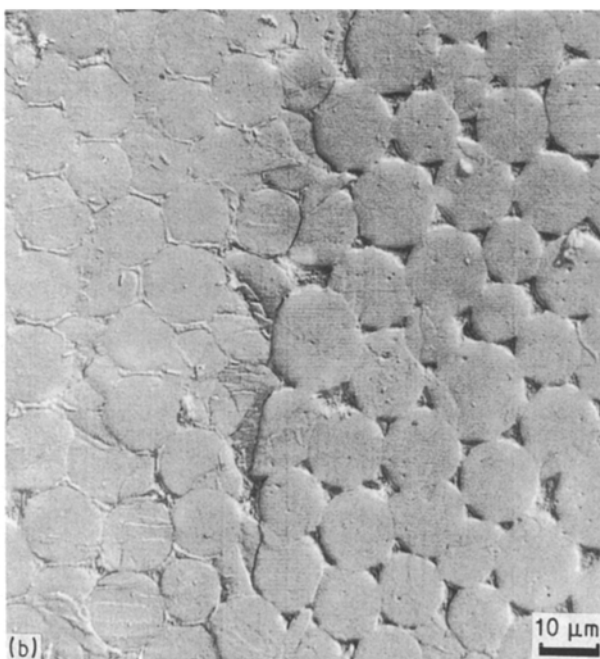


Figure 1 (a) Surface cut perpendicular to the fibres, not etched. Optical micrograph taken in reflection using Nomarski contrast; for A, B and C see text. (b) Similar to (a), with a marked boundary between two regions of different inclination of fibres.

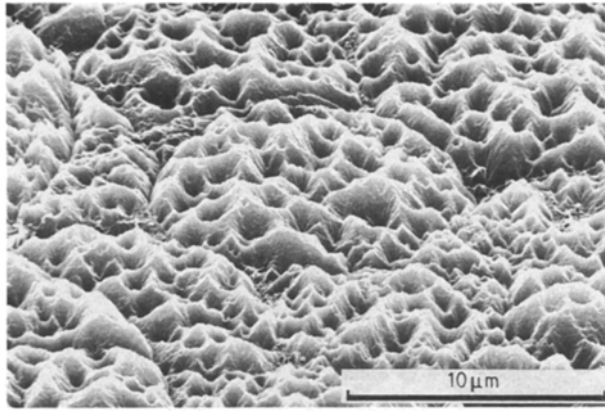


Figure 2 Scanning electron micrograph of specimen cut perpendicular to the fibres and etched, tilted  $60^\circ$  around a horizontal axis.

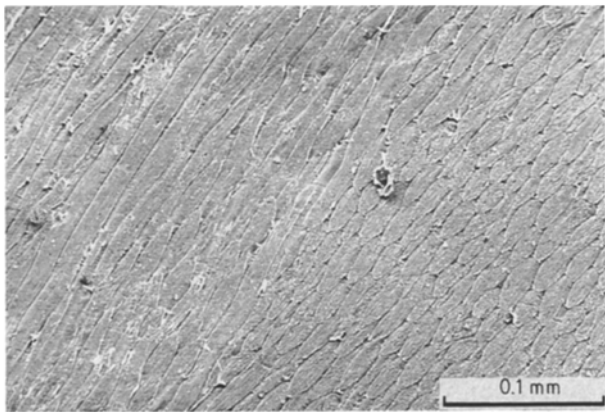


Figure 3 Scanning electron micrograph of specimen cut longitudinally and etched, tilted  $60^\circ$  around a horizontal axis.

typically  $\sim 12^\circ$  and sometimes as much as  $17^\circ$  out of the plane of the specimen. Such variations in orientation confirm the conclusions of the previous paper [1], inferred from the widths of X-ray reflections. A further implication is that adjacent pairs of fibres frequently are relatively misaligned because they reveal different aspect ratios. It follows that it will not be possible to bond two misaligned fibres together without the intervention of crystallographic defects such as twist boundaries. Such defects are likely to etch preferentially and the boundaries between two welded fibres to be correspondingly demarcated. It is a feature of Fig. 3 that virtually all interfibrillar boundaries are marked after etching. This point will be returned to below in the context of the lateral cohesion of the compacted fibre composite.

### 3.3. Recrystallized lamellae

The lamellae formed by melting part of the original fibres and subsequent recrystallization are readily identified in longitudinal sections such as Fig. 4, appearing in extensive regions lying parallel to and between the remaining fibres. They are not, however, restricted to interstices between fibres; some lamellae have recrystallized within the original fibres as is evident from low-magnification images. Such regions

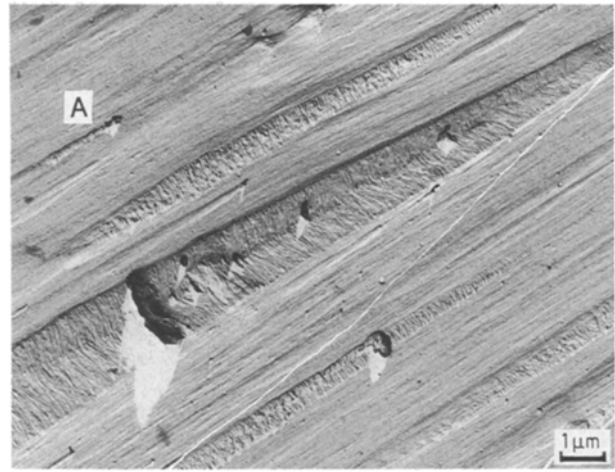


Figure 4 Transmission electron micrograph of etched longitudinal section showing fibres and recrystallized material both between and within them.

can be very small; that near A in Fig. 4 is only  $2\ \mu\text{m}$  long and  $\sim 0.1\ \mu\text{m}$  wide. More typically, widths are of the order of  $1\ \mu\text{m}$ .

Selective melting may, in principle, arise in one of two ways. The melted regions may have had an inherently lower melting point (because of thinner lamellae and/or concentrated lower molecular weight polymer, for example). Alternatively, the melting point of the remainder could have been raised because of the constraints of a highly oriented system. While the possibility of a lower melting surface layer on the fibres cannot be excluded on present evidence, the latter explanation seems the more probable in view of the detailed morphology. The melting point for highly oriented systems is known to be raised because the amorphous phase is constrained to be oriented rather than random. As a consequence, the entropy of the melt is lowered which gives, in turn, a decreased entropy of fusion and so an increased melting point. In a complex system such as that under consideration, the regions of lowest melting point will be those where there is least constraint, so that the molten phase can randomize more easily. These are the outer surfaces next to an interstice together with any internal defective regions possessing sufficient free volume. In Fig. 4 the widest region of lamellae fills what was an interfibrillar interstice but neighboring regions of recrystallized layers are legacies of internal texture. In all cases the habit of the recrystallized lamellae indicates that they formed in strain-free conditions, i.e. from a random melt.

The existence of a characteristic intrafibrillar texture, made up of quasi-cylindrical regions, typically  $0.5\ \mu\text{m}$  diameter, as identified in Fig. 4, is confirmed by Fig. 5. In the centre, the plane of cutting has intersected a fibre at an angle so that the internal cylinders are seen in elliptical section, each with a black thread at its head. These threads are an artefact of replication. They are the legacy of the first-stage replicating film entering a deep cavity, opened by this particular etchant, but then being incompletely removed from the carbon film in the second stage. In the left centre of

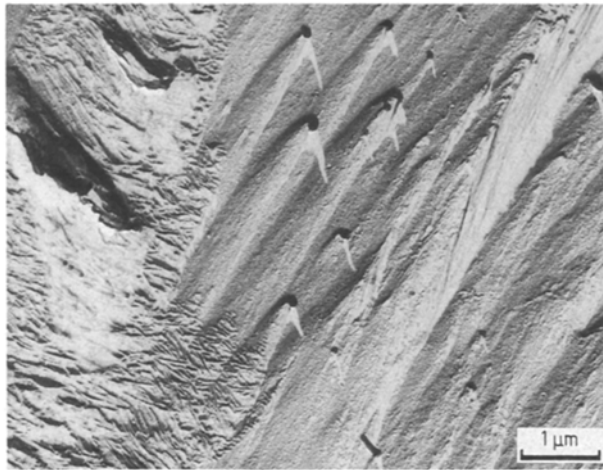


Figure 5 Transmission electron micrograph of etched longitudinal section showing a region where fibres are significantly inclined to the cutting direction. Note the modulation of recrystallized lamellae by the defective regions within the fibre.

Fig. 5, four of the ellipses interact with the recrystallized lamellae, which are modulated by the elliptical boundaries. This shows that the ellipses (and the cylinders which they represent) are genuine textural features which were present within the fibres before recrystallization. Also in Fig. 5, there are lamellae decorating several ridges running diagonally from the top right. These, too, are probably linked to the polymer having had sufficient free volume in which to melt.

We may now make a link between these cylindrical intrafibrillar defects and the craters etched into the end surfaces of fibres. In Fig. 6 long threads of replicating film have survived to reveal the presence of deep cylindrical holes etched out, along the fibre axis, at the centre of each crater. The formation of such deep holes is independent confirmation of the presence of regions of enhanced penetration of the etchant and greater free volume. The craters themselves presumably result from a subsequent widening around the initial holes by the etchant as it penetrates further into the fibre. This is borne out by the manner in which the outer surfaces of the fibres are eaten back to a similarly chamfered edge. This effect is visible in Fig. 6 but is seen particularly well, with a different etchant, in Fig. 9. The action of the etchant is, therefore, prone to exaggerate the diameter of the cylindrical regions giving the craters but not their number; this is approximately 50 per 10 µm diameter cross-section, i.e. approaching  $1 \mu\text{m}^{-2}$ .

When lamellae begin to form they do so in the presence of fibres which have partly melted to leave surfaces in prime condition to nucleate subsequent growth. When this occurs, lamellae will, therefore, adopt the orientation of the fibre at the nucleation site and grow outwards from it. All these phenomena can be demonstrated from the details of the consequent microstructure.

Firstly, the appearance of lamellae at higher resolution shows them to be viewed edge-on when the fibres lie in the plane of the photograph (Figs 4 and 8). In any one instance this implies that the chain axis,  $c$ ,

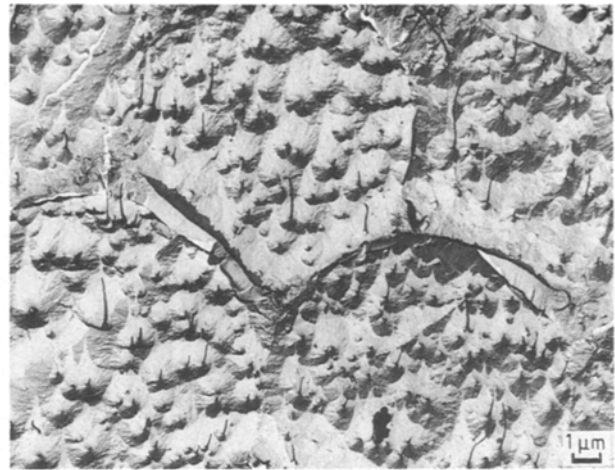


Figure 6 Transmission electron micrograph of etched transverse section showing fibre sections and recrystallized material in the interstices.

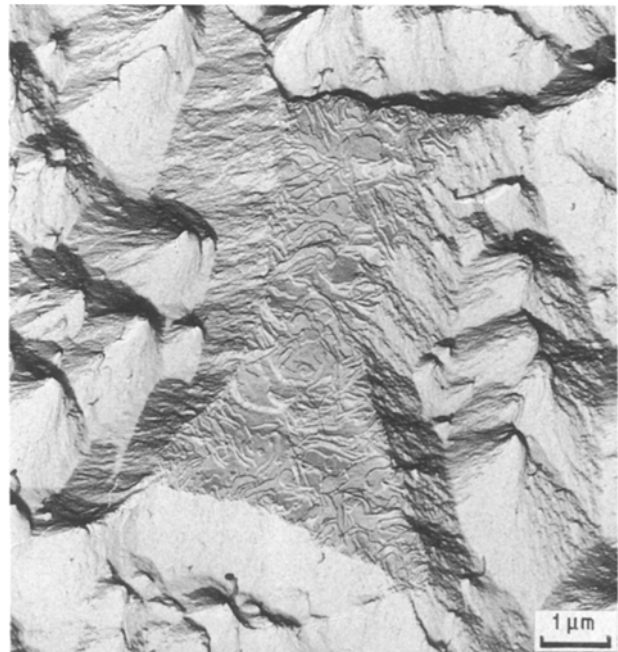


Figure 7 Magnified view down the fibre direction of lamellae crystallized in the interstice between four fibres.

itself lies in the page. But as this is true in every case it follows that there is cylindrical symmetry and that the chain axis in the lamellae is parallel to the fibre axis.

Secondly, views near B in Fig. 4 (seen in detail in Fig. 8 of the previous paper) clearly show two sets of lamellae each continuous with the adjacent fibre, having grown out from the fibres and met approximately mid-way. In a plan view, Fig. 7, the shape and direction of the exposed prism surfaces can be used as indicators of the growth direction, which is always  $b$  for melt growth. From these indications it appears both that the same lateral orientation can persist over distances of a micrometre or more and that lamellae which are vertically adjacent do not always have the same orientation. Both observations are consistent with growth occurring from a limited number of nuclei as is characteristic of growth at low supercoolings.

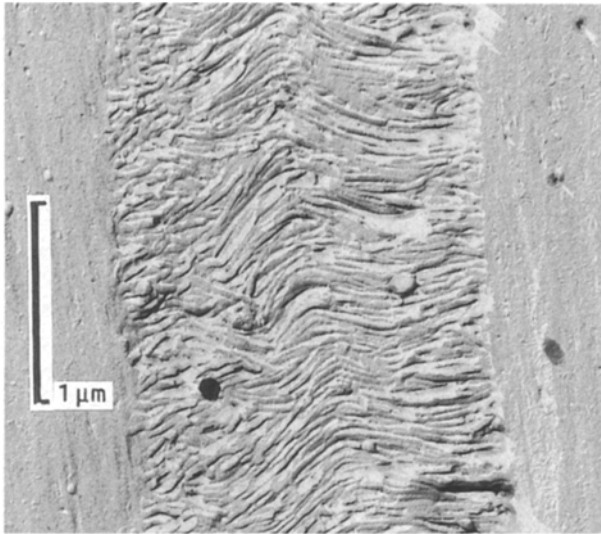


Figure 8 Longitudinal section of interstice; the lamellar details identify the lamellae as growing in three different directions from three distinct fibres, under strain-free conditions.

Consideration of lamellar shapes seen in elevation leads to the same conclusion. We can be confident from the treatment temperatures and pressures used that lamellar crystallization did not occur until the final cooling. The internal evidence, e.g. from Fig. 4, is of lamellae which are usually straight in projection, i.e. planar, which is an indication for linear polyethylene of crystallization at low supercooling, approximately but not exactly within Regime I [4]. Quite commonly one has two sets of lamellae, each growing in from the fibre boundary and meeting in the middle, as discussed above, often with an indication of a slight mismatch of orientation such as would result from different crystallographic orientations on either side of an interstice. Plan views such as in Fig. 7 tend to confirm that an arbitrary longitudinal section will intersect just two sets of lamellae. Less often, in the centre of a cavity, more than two sets of lamellae can be intersected. Fig. 8 is particularly revealing in this respect. Here one set of lamellae with straight outlines has grown in from the right surface and a second set began growing from the left surface at an angle to the page. In the middle, lamellae with curved and S-shaped profiles with central  $\{201\}$  surfaces are evident whose profile shows that they would have been growing normal to the page. Curved profiles are uncommon in this sample but show where growth has occurred in Regime II [4]. In general, therefore, we can infer that crystallization has occurred during cooling at temperatures close to the change of kinetic regime, i.e.  $127^\circ\text{C}$  for linear polyethylene [5].

### 3.4. Lateral interfaces

The good transverse properties of the compacted material are an indication that effective links have been established within the resulting fibre/lamellar composite. Further details of these can now be added to the general features described earlier. Thus Fig. 9 shows its central fibre making five interfibrillar con-

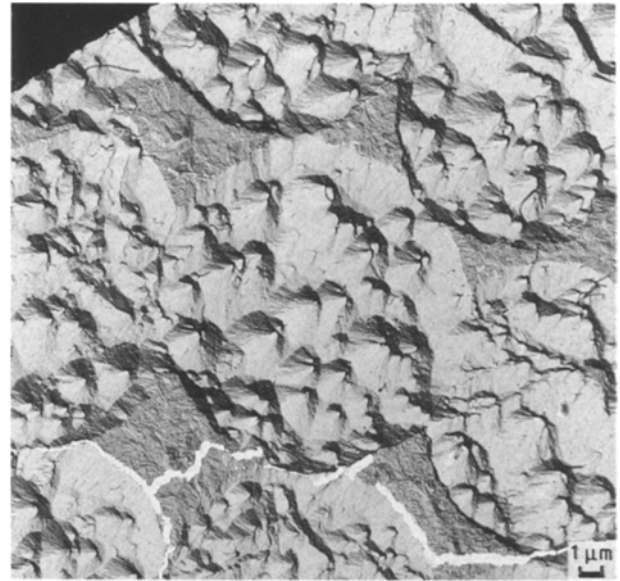


Figure 9 Transverse section showing three fibres in a row, welded at their junctions.

tacts. That at 12 o'clock is actually separated by a thin vein of intervening lamellae. Of the other four, the adjacent fibres have deformed substantially to fit the profile of the central fibre in three cases, with the central fibre itself deforming slightly at 2 o'clock. In every case the interfibrillar boundary can still be traced implying, in line with earlier discussion, that the contact has some degree of imperfection allowing enhanced etching.

Fig. 6 shows two cases where interfibrillar contacts have yielded, drawing material between the two separated fibres. This must have happened after the lamellar crystallization, otherwise the deformed regions would themselves have recrystallized. In Figs 6 and 9 there are examples of fibres which have deformed substantially, presumably during the application of pressure. That to the right of the central fibre in Fig. 9 has gross faults running from the interfibrillar contact zone to a central point (or line in projection). Any weaknesses so introduced would, however, have had the chance to heal by melting and recrystallization in the later stages of the process.

The fibre/lamellar bond is, in principle, as strong as intrafibrillar binding because both will reflect the properties of the unit cell provided contacts are crystallographic, which is guaranteed by the nucleation of lamellae on the fibres. The integrity of the connection, with no weakness to the etchant, is very evident in Fig. 10. This property and the resistance of chain-folded lamellae to fibrillation are principal reasons why the properties of the compacted composite are comparable with those of the starting fibres.

Fig. 10 also shows detail within the fibres themselves, even with an etchant which is not the best for this purpose. There is a semblance of a periodicity on the same scale as the thickness of the adjacent lamellae. It is possible that this reflects embryonic melting and recrystallization within the body of the fibre. Nevertheless, other (unpublished) work has shown that intrafibrillar structure in ultra-stiff polyethylene fibres

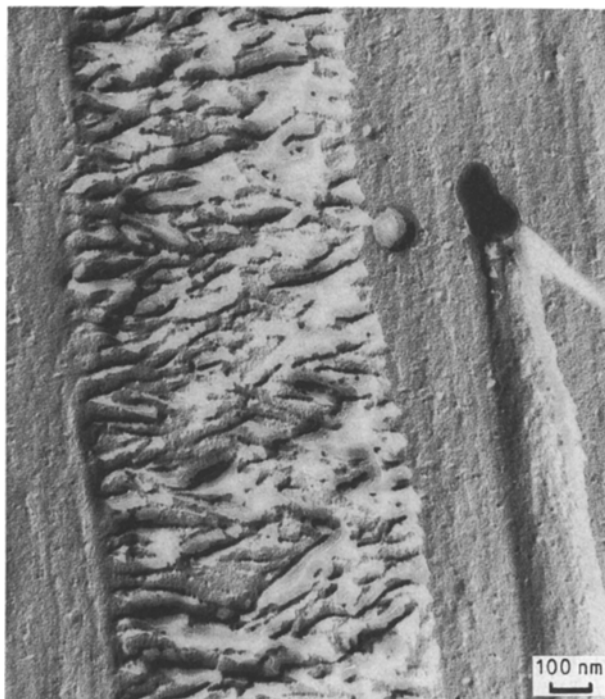


Figure 10 Fine detail of interstitial material, fibre material, and the connection between them.

can be well resolved with suitable etchants. As the compacting process is applicable to fibres of different properties there are now good prospects of being able to relate mechanical properties to underlying fibrillar microstructure.

#### 4. Conclusions

1. Microscopic examination of the internal micro-

structure of compacted polyethylene composites has revealed irregular packing of fibres, many of them having undergone severe deformation, with lamellae filling all interstices. The degree of misalignment between fibres can be measured and may be  $10^\circ$  and more.

2. At  $138^\circ\text{C}$ , melting (and recrystallization) only occurs in regions where molten polymer is not constrained to remain oriented. This happens mostly between, but also within, fibres. Internally it occurs in quasi-cylindrical regions, typically  $\sim 1\ \mu\text{m}$  diameter, which possess enhanced free volume. These are an unsuspected feature of the original fibres.

3. Lamellae form from molten polymer in strain-free conditions, but share the *c* axis orientation of the fibres on which they nucleate, thereby bringing good lateral properties to the resulting composite.

#### References

1. P. J. HINE, I. M. WARD, R. H. OLLEY and D. C. BASSETT, *J. Mater. Sci.* **28** (1993) 0000.
2. R. H. OLLEY and D. C. BASSETT, *Polymer* **23** (1982) 1707.
3. J. H. M. WILLISON and A. J. ROWE, "Replica, Shadowing and Freeze-Etching Techniques" (North Holland, Amsterdam, 1980).
4. D. C. BASSETT, A. M. HODGE and R. H. OLLEY, *Proc. Roy. Soc. A* **377** (1981) 39.
5. J. D. HOFFMANN, G. S. FROLEN, G. S. ROSS and J. I. LAURITZEN, *J. Res. Nat. Bur. Stand. A* **79** (1975) 761.

Received 23 April  
and accepted 2 June 1992